Seasonal changes of sources and volatility of carbonaceous aerosol at urban, coastal and forest sites in Eastern Europe (Lithuania)

Masalaite, A.; Remeikis, V.; Zenker, K.; Westra, Dineke; Meijer, H. A. J.; Dusek, U.

Published in:
Atmospheric environment

DOI:
10.1016/j.atmosenv.2020.117374

Publication date:
2020

Atmospheric Environment 225 (2020) 117374

Contents lists available at ScienceDirect

Atmospheric Environment

journal homepage: http://www.elsevier.com/locate/atmosenv

Seasonal changes of sources and volatility of carbonaceous aerosol at urban, coastal and forest sites in Eastern Europe (Lithuania)

A. Masalaite [a,*], V. Remeikis [a], K. Zenker [b], I. Westra [b], H.A.J. Meijer [b], U. Dusek [b]

[a] State Research Institute Center for Physical Sciences and Technology, Vilnius, Lithuania
[b] Centre for Isotope Research (CIO), University of Groningen, Groningen, the Netherlands

HIGHLIGHTS

- ^{13}C signature of organic aerosol reveals main sources.
- Isotopic composition shows seasonal difference.
- $\delta^{13}C_{OC}$ change via kinetic fractionation.

GRAPHICAL ABSTRACT

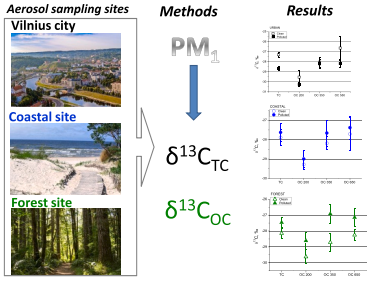

ARTICLE INFO

Keywords:
Aerosol
Isotopic composition
IRMS

ABSTRACT

We measured stable carbon isotope ratios of total carbon (TC) and organic carbon (OC) in fine carbonaceous aerosol fraction sampled in August and September 2013 at urban, coastal and forest sites in Lithuania. $\delta^{13}C$ values of TC for all three sites over the whole measurement period varied from −29.3 to −26.6‰, which is in the range of particles emitted by fossil fuel combustion in Eastern Europe. The isotopic composition at the forest and coastal site showed a similar variation during two contrasting pollution periods. $\delta^{13}C$ values in the clean period were more variable, whereas the polluted period was characterized by a gradual enrichment in $\delta^{13}C$ compared to the clean period. In the polluted period air masses originated from southern, southeastern or southwestern direction, indicating long-range transport of pollutants from Eastern Europe and Southern Europe to Lithuania. Oxidative processing during long-range transport or the different source signatures (e.g., enriched ^{13}C signature of gasoline used in Western Europe vs. Eastern Europe) could cause the less negative $\delta^{13}C_{OC}$ values during the polluted episode. $\delta^{13}C$ for OC desorbed from the filter samples was separately measured during three different temperature steps (200 °C, 350 °C and 650 °C). OC desorbed at 200 °C had the most depleted ^{13}C signature of around −29‰ at all three sites.

A comparison with previously published data measured during the winter at the same sites showed that both TC and OC had less negative $\delta^{13}C$ values in winter than in summer, which can be explained by the contribution of biomass/coal burning sources in winter. At the urban site $\delta^{13}C$ of OC did not change much with increasing desorption temperature in winter, which is typical for primary sources, but in the summer $\delta^{13}C$ of OC was depleted for lower desorption temperatures, possibly due to the influence of SOA formation. A higher fraction of more refractory OC in summer compared to winter-time suggests active photochemical processing of the primary organic aerosol as an important process at all three sites.

* Corresponding author.
E-mail address: agne.masalaite@ftmc.lt (A. Masalaite).

https://doi.org/10.1016/j.atmosenv.2020.117374
Received 16 August 2019; Received in revised form 18 February 2020; Accepted 24 February 2020
Available online 28 February 2020

1. Introduction

Aerosols have an effect on the Earth's climate e.g. (Ceburnis et al., 2016; Jimenez et al., 2009; Pöschl and Shiraiwa, 2015; Shiraiwa et al., 2017; Viana et al., 2014), and human health (Butt et al., 2016; Pöschl, 2005). Therefore there is a strong scientific interest to investigate the sources and atmospheric formation processes of atmospheric aerosols. A significant fraction (20–90%) of atmospheric aerosols consists of carbonaceous compounds (Jacobson et al., 2000; Jimenez et al., 2009), of which the major sources are primary emissions from fossil fuel (FF) combustion, especially in urban areas (Cao et al., 2011; Dusek et al., 2013b; Masalaite et al., 2015; Szidat et al., 2006), biomass burning (BB), often dominant in rural areas (Sang et al., 2012; Schurman et al., 2015b), primary biogenic aerosol emitted in forest areas (Miyazaki et al., 2012; Schumacher et al., 2013) and secondary formation in the atmosphere through oxidation of anthropogenic or biogenic precursor gases (Hallquist et al., 2009; Schurman et al., 2015a). The chemical complexity of the carbonaceous aerosol fraction makes source apportionment challenging. Numerous studies have been conducted in different locations worldwide to gain insight into sources and properties of the carbonaceous aerosol. Due to the relatively short life-time of aerosols (in the order of 1–2 weeks), their characteristics and sources can vary strongly in space and time, resulting in regional differences (Putaud et al., 2004, 2010; Viana et al., 2014) as well as distinct seasonal variations (Dusek et al., 2017; Kundu et al., 2010; Miyazaki et al., 2012; Ni et al., 2018; Sun et al., 2015; Vodička et al., 2019; Zhang et al., 2013, 2018). Residential heating, traffic emissions and limited photochemical processing have a major influence on aerosol properties during winter-time in various European locations (Crippa et al., 2013; Garbaras et al., 2018; Masalaite et al., 2017; Pirjola et al., 2017; Theodosi et al., 2018).

Total carbon (TC) in atmospheric aerosols is operationally subdivided into organic carbon (OC) and elemental carbon (EC) fractions. EC is produced from incomplete combustion of fossil fuels and biomass (Bond et al., 2007) and is chemically relatively inert after emission. For OC, the main primary emission sources are fossil fuel combustion and biomass burning (in line with EC emissions) as well as primary biogenic aerosol, such as pollen, spores or plant debris. Moreover, secondary formation from biogenic and anthropogenic precursor gases constitute a major and in some locations the dominant fraction of OC (Hallquist et al., 2009; Jimenez et al., 2009; Zhang et al., 2007). In addition, OC is affected by various degrees of modification through photochemical processing, after it is emitted to or formed in the atmosphere (Hallquist et al., 2009).

The carbon isotopic composition (i.e., the $^{14}C/^{12}C$ and $^{13}C/^{12}C$ ratio) of total carbon and of separate carbon fractions has been analyzed in a number of recent studies (Ceburnis et al., 2016; Kirillova et al., 2010; Martinsson et al., 2017; Vodička et al., 2019). The $^{14}C/^{12}C$ ratio is useful to distinguish the contributions of fossil fuel emissions and non-fossil components to the aerosol carbon, because of the absence of ^{14}C in fossil fuels that is due to the half-life of ^{14}C of 5730y. The stable carbon ratio $^{13}C/^{12}C$ can for example be used to differentiate marine versus continental sources (Chesselet et al., 1981; Pavuluri et al., 2011) or biogenic or biomass burning sources from C3 and C4 plant types (Ballentine et al., 1998; Mkoma et al., 2014). It can also give indication of the extent of oxidative processing of the organic matter (Aggarwal and Kawamura, 2008; Pavuluri et al., 2011; Zhang et al., 2016). Most carbonaceous aerosol sources in Europe originate from C3 plants, and those derived from fossil fuel mostly have a similar $\delta^{13}C$ signature. Therefore, the stable carbon isotope ratio values of various sources overlap to some extent, but regionally some sources can be distinguished: e.g. coal tends to be enriched in ^{13}C compared to particles from liquid fossil fuel combustion (Widory, 2006).

Several studies are reported with successful use of carbon isotope ratios as a tracer to identify and apportion pollution sources (Dusek et al., 2013b, 2017; Fisseha et al., 2009a; Kirillova et al., 2010; Martinsson et al., 2017; Masalaite et al., 2015; Szidat et al., 2006; Widory et al., 2004). Dusek et al. (2017) showed that the main source categories of carbonaceous aerosols at a regional background site in the Netherlands are fossil fuel combustion, biomass burning and biogenic secondary organic aerosol material (SOA). Fisseha et al. (2009a) determined $\delta^{13}C$ values of the different aerosol fractions (water soluble organic carbon (WSOC), water insoluble organic carbon (WIOC), carbonate and black carbon) and found that WSOC is enriched in ^{13}C compared to other fractions and contributed about 60% to the total carbon mass. Kirillova et al. (2010) indicated that WSOC in ambient Stockholm aerosols was 88% of contemporary biogenic C3 plant origin. Other isotope-based studies confirmed that OC is mostly from non-fossil sources, determined importance of biogenic SOA (BSOA) and revealed the importance of BB in winter (Szidat et al., 2009). Most European source apportionment studies to date have focused on Western Europe. However, sources of carbonaceous aerosols in Eastern Europe can differ from Western Europe (Górka et al., 2014; Masalaite et al., 2012; Widory, 2006; Widory et al., 2004) and more studies in this region are needed. Source apportionment using ^{13}C was not very successful in Western Europe, because the main sources overlap (Martinsson et al., 2017). On the other hand, due to the different isotopic signatures of coal burning, liquid fuel combustion and biomass burning (Garbaras et al., 2015; Masalaite et al., 2017, 2018; Widory, 2006) in Eastern Europe, stable isotopes can be useful in source apportionment in this region. A few previous studies on stable carbon isotope ratios in ambient aerosols have been conducted in the Baltic region (Garbaras et al., 2018; Garbarienė et al., 2016; Masalaite et al., 2017, 2018). The main findings of these studies were that the dominant pollution sources during winter-time are fossil fuel combustion and biomass burning, with biomass-derived particles having a dominant contribution to the mass concentration of carbonaceous matter (up to 84%). The most detailed study to date by Masalaite et al. (2018) investigated carbonaceous aerosol sources depending on particle size and volatility and concluded that the more volatile carbon fraction of the smallest particles ($D_{50} < 0.18$ μm) originated almost entirely from fossil fuels, whereas the more refractory carbon fraction in the large size range ($0.32 < D_{50} < 1$ μm) was largely originating from biomass burning at an urban site. Shipping emissions were linked to OC strongly depleted in ^{13}C observed at a coastal site with $\delta^{13}C$ values down to −31‰.

So far most of the studies in this region have been conducted during winter-time. However, the properties and sources of carbonaceous aerosols during summer time are much more complex due to the stronger input of biogenic sources, stronger secondary aerosol formation as well as photochemical aging processes (Aggarwal et al., 2013; Pan et al., 2018; Sun et al., 2012). The objective of the current study is to investigate the stable carbon isotopic composition of organic aerosol during summer time. We investigate the stable carbon isotopic composition of fine aerosol particles collected during summer and early fall at urban, coastal and forest sites in Lithuania. By studying $\delta^{13}C$ values in different volatility fractions of the organic aerosol, we aim to gain insight into formation and aging mechanisms of the organic aerosol. A comparison with winter-time data from the same sites measured in previous studies allows to draw conclusions about seasonal changes in aerosol sources.

2. Methods

2.1. Aerosol sampling and sampling sites

Aerosol filter samples were collected at three sites (urban, coastal and forest) in Lithuania in August and September 2013. The fine particle fraction (PM_1, $d_p < 1$ μm) of atmospheric aerosol was collected using high-volume samplers (500 L/min) onto Pallflex quartz fiber filters (150 mm diameter). The automated filter change each 24 h was performed at the coastal and forest site (Digitel DHA–80) but varied between 1 and 3 days at the urban site, where a manual filter change system was

employed (Digitel DH–77). Before sampling, all filters were pre-heated for 24 h at 550 °C to avoid possible adsorbed organic contaminants. All filters were wrapped individually in clean aluminum foil and stored at −20 °C from the end of sampling until analysis, except during transport to and from the sampling sites. Blank filters were treated exactly like the sample filters, except that no aerosols were collected on them.

All three sampling locations are described in detail by Masalaite et al. (2017). In short, the location is an urban background site in the capital city of Lithuania (Vilnius 54° 64′ N, 25° 18′ E). The coastal site (55° 38′ N, 21°, 03′ E) is the air pollution monitoring station in Preila (on the Curonian Spit), which is a representative coastal background site. The forest location is an ecological monitoring station located by a lake in Rugsteliskis (55° 46′ N, 26°, 00' E), surrounded by a boreal and Scots pine tree forest (Fig. 1).

Meteorological parameters (air temperature, pressure, precipitation, wind speed, wind direction) were recorded during the sampling period at all three locations. Isobaric air mass back trajectories were calculated for 24 h and 48 h prior to the sampling at a height of 500 and 300 m a.s.l. with a new trajectory starting every 4 h using the HYSPLIT model (Stein et al., 2015) (all air mass back trajectories are provided in supporting material). Air masses from west and/or north were dominant during August and the first period in September (09 01–09 09), while southern, southeastern or southwestern direction air masses were occurring during the second period in September (09 10–09 16). Due to the different TC mass concentrations and according to the classification presented in Ovadnevaitė et al. (2007), the first period is named "clean" (air masses from the North Atlantic Ocean, the Norwegian Sea and Northern Europe), whereas the second period is called "polluted" (influence from Eastern Europe and Southern Europe) in the rest of the manuscript.

The meteorological parameters as average temperature of the day (24 h), sunshine hours, wind speed, wind direction and rainfall were measured at the measurement site.

2.2. Analysis of stable carbon isotope ratios in total and organic carbon fractions

Stable carbon isotope ratios of total carbon ($\delta^{13}C_{TC}$) are expressed on the Vienna Pee Dee Belemnite (VPDB) scale and were measured using sample material from a round punch (1.9 mm in diameter) of the quartz fiber filter. This filter piece was wrapped into a tin capsule and introduced into an elemental analyzer (Flash EA 1112) connected to a continuous flow stable Isotope Ratio Mass Spectrometer (IRMS, Thermo Finnigan Delta Plus Advantage). A caffeine external reference material

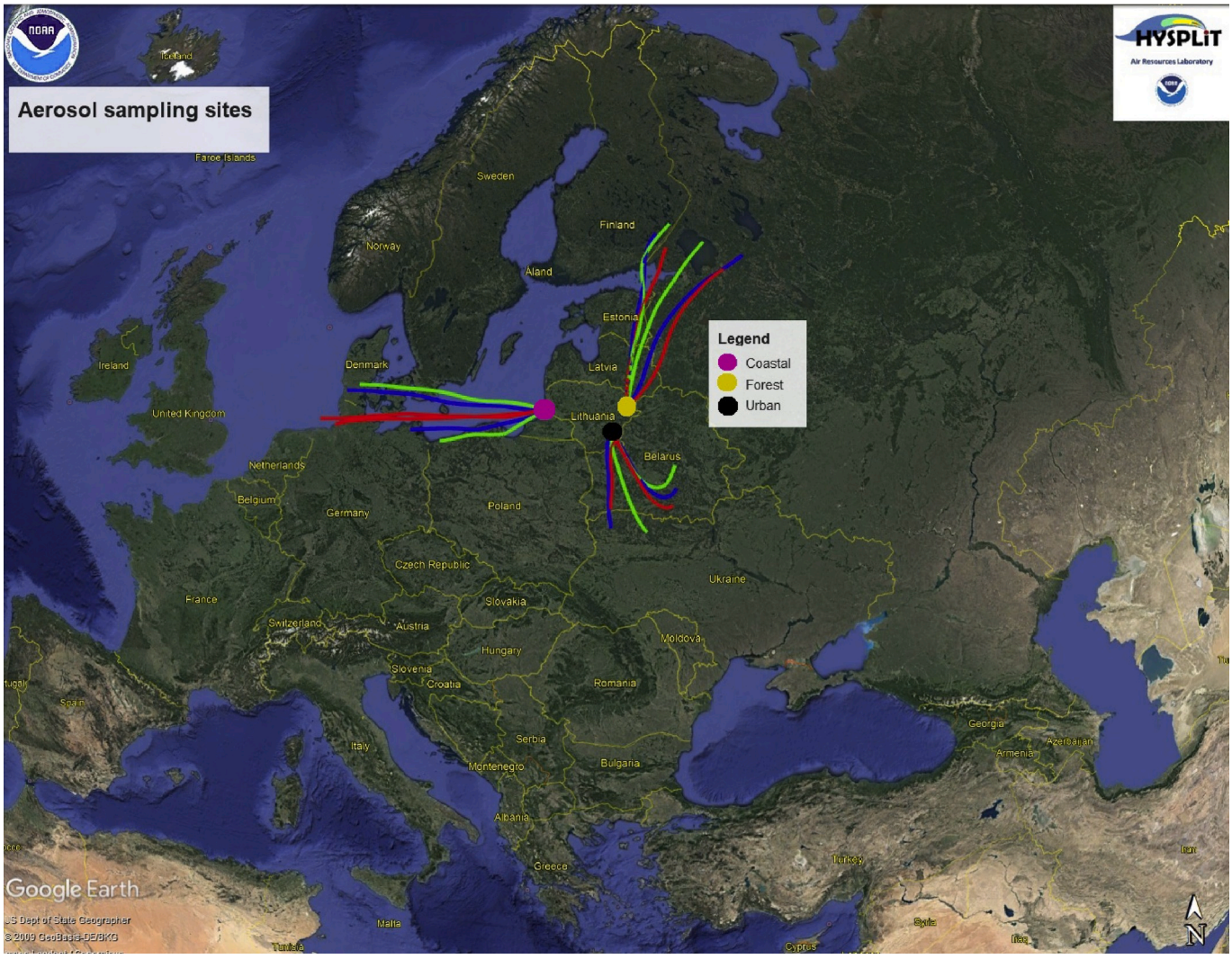

Fig. 1. The three sampling locations coastal (purple dot), forest (yellow dot) and urban (black dot) location. Also shown are isobaric air mass back trajectories generated by NOAA (Stein et al., 2015) using the "Google Earth" application representing typical examples of west (coastal site 01 09 2013), north (forest site 05 09 2013) and south-east (urban 10 09 2013) air mass types. The 24 h back trajectories were calculated at a height of 500 m a.s.l. with a new trajectory starting every 4 h. (For interpretation of the references to colour in this figure legend, the reader is referred to the Web version of this article.)

($\delta^{13}C_{TC} = -27.77 \pm 0.04$‰ with respect to VPDB) was measured every day for calibration. All samples were measured in duplicate and the standard deviations (‰) of the two measurements (in fact $\frac{1}{2}\sqrt{2}$times their difference) are reported as the error bar of $\delta^{13}C_{TC}$. Details of $\delta^{13}C_{TC}$ measurements are described in previous studies (Garbarienė et al., 2016; Masalaite et al., 2017).

Stable carbon isotope ratios of organic carbon ($\delta^{13}C_{OC}$) were measured using a thermal–desorption isotope ratio mass spectrometry (IRMS) system developed at Centre for Isotope Research (CIO) in Groningen, based on the system described by Dusek et al. (2013a). This system consists of a commercially available OC-EC analyser (Sunset Inc.) connected to a continuous flow IRMS (Micromass, now Isoprime Optima) via a custom-made interface. A filter punch is placed in the front-oven of the Sunset OC-EC analyzer, where the temperature is changed in three steps from 200 °C, via 350 °C–650 °C. The organic compounds desorbed at each temperature step are catalytically converted to CO_2 in the back oven of the Sunset analyzer. The CO_2 sample is sequentially collected in two liquid N_2 traps (an initial and a focus trap) and separated from possible traces of N_2O and NO_2 using a GC column. It is introduced into the Optima via a custom-made open split interface. Reference materials (A caffeine reference with $\delta^{13}C = 37.7$‰ and an oxalic acid reference 'C7'with $\delta^{13}C = 14.5$‰) are measured at the beginning, in the middle and at the end of each measurement day, by placing a small amount of an aqueous solution of the reference material on a clean quartz fiber filter, which is subsequently introduced into the OC-EC analyzer, dried and thermally desorbed at 650 °C. A detailed description of the measurement system and analytical procedure is provided by Zenker et al. (2020). The organic compounds desorbed at each temperature step (200 °C, 350 °C and 650 °C) will be denoted as "OC,200", "OC,350" and "OC,650" and the isotopic composition as $\delta^{13}C_{OC,200}$, $\delta^{13}C_{OC,350}$ and $\delta^{13}C_{OC,650}$, respectively, in the rest of the manuscript.

The method used for removal of carbonate carbon is based on the NIOSH method 5040 with minor modifications (Kawamura et al., 2004; Zhang et al., 2014). Filter punches were treated with HCl vapor as follows. Each filter punch was placed in a glass Petri dish and moved to the bottom of a glass desiccator, where a glass with HCl was introduced. The filters were exposed to HCl vapor in the desiccator for one hour. Excess HCl was removed from the sample by replacing the glass with HCl by a glass containing NaOH pellets. The filters with removed carbonate carbon were analyzed for TC concentration as well as their isotopic ratios, as described above.

3. Results and discussion

3.1. Summer time data

Fig. 2 presents $\delta^{13}C$ values of TC for all three sites over the whole measurement period. $\delta^{13}C_{TC}$ values vary from -29.4 ± 0.1‰ to -26.6 ± 0.4‰ at the urban site (average -27.6 ± 0.8‰), from -28.5 ± 0.1‰ to -27.2 ± 0.2‰ at coastal site (average -27.8 ± 0.5‰) and from -28.7 ± 0.2‰ to -26.9 ± 0.2‰ at the forest site (average -27.9 ± 0.5‰). All $\delta^{13}C_{TC}$ values vary within ~2‰. Most reported values lie broadly in the range of particles emitted by liquid fossil fuel combustion in Eastern Europe (-28 ± 0.9‰) (Masalaite et al., 2017). The most negative reported isotopic values overlap with $\delta^{13}C$ of natural source of aerosol like α-pinene (Haberstroh et al., 2019) and β-pinene (Fisseha et al., 2009b). This is not surprising considering the fact that higher VOC emissions from terrestrial plants are observed during summer, especially at forest sites, as was reported by Martinsson et al. (2017). Meusinger et al. (2017) reported that Secondary Organic Aerosol (SOA) formed from α-pinene was only slightly enriched compared to the precursor VOC, after all the α -pinene has reacted. Therefore SOA from short-lived precursors can still reflect the isotopic signature of the precursor VOC. Some isotope values are more enriched. We should note that the $\delta^{13}C$ values of α and β -pinene naturally produced by plants is still uncertain. Haberstroh et al. (2019) provided $\delta^{13}C$ values of typical monoterpenes emitted by *Q. suber* and *C. ladanifer*, a shrub and a tree species, which varied in the range from −27 to −35‰, with more enriched values corresponding to draught conditions. They also found that emitted monoterpenes were depleted in ^{13}C compared to the biomass by several ‰. $\delta^{13}C_{TC}$ values above −27.0‰ were previously attributed to the biomass burning materials reported by Garbaras et al. (2015). However, biomass burning and coal burning emissions used for domestic heating is minor to the main aerosol particles budget during summer time in Europe (Puxbaum et al., 2007; Zielonka et al., 2005). Pollutants derived from coal burning with $\delta^{13}C$ values between −21‰ and −25‰ (Widory, 2006) can be transported from regions where coal is used all year round,

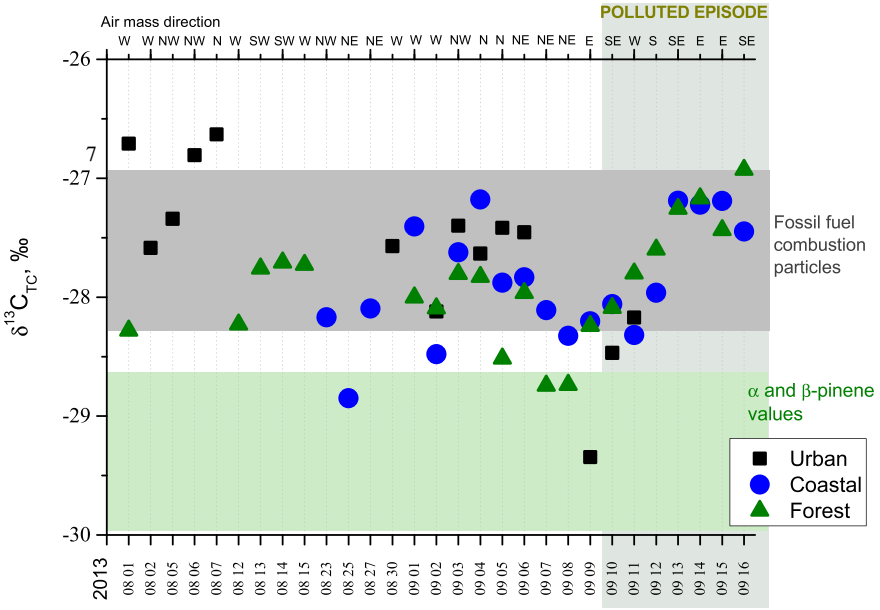

Figure 2. $\delta^{13}C_{TC}$ of samples from urban, coastal and forest sites over the whole measurement period. The horizontal shading area denotes the $\delta^{13}C$ range for the specific carbonaceous sources: value of liquid fossil fuel combustion from Masalaite et al. (2015) and value of β-pinene taken from Fisseha et al. (2009b) and α-pinene taken from Haberstroh et al. (2019), while the vertical shading area (from 10 to 16 September) denotes a polluted episode.

but this contribution is likely to be small (Zielonka et al., 2005). Other possible sources are SOA from different plant precursors (Miyazaki et al., 2012), or long-range transport from Western Europe, where liquid fuels have an enriched isotopic signature compared to Eastern Europe (Masalaite et al., 2017; Widory, 2006). Moreover, during long-range transport oxidative processing can result in an enriched isotopic signature in the OC remaining in the aerosol phase (Aggarwal and Kawamura, 2008). Most likely explanation is a combination between the last two.

Fig. 2 (above x axis) presents the air masse directions that were dominant at all three receptor sites at the same day. The air masses from the clean West and North sector are advected over the North Atlantic Ocean, the Norwegian Sea and Northern Europe and are in general less influenced by anthropogenic sources such as petrol and diesel burning emissions, oil and coal combustion (Swietlicki, 1989). The averaged $\delta^{13}C_{TC}$ values were ~0.5‰ lower during the clean period than during the polluted one for the forest and coastal site.

A survey of the data showed strongly enriched $\delta^{13}C_{OC,650}$ values down to −21‰ in some samples at the urban site. The strong enrichment in ^{13}C at 650 °C was unexpected for the PM_1 fraction. Strongly enriched $\delta^{13}C_{OC,650}$ values suggested the contribution of a specific sources with high $\delta^{13}C$ values. Pollutants derived from coal burning shows $\delta^{13}C$ values between −21‰ and −25‰ (Widory, 2006), however, coal burning should not be strong source in summer. On the other hand, calcium carbonates, whose $\delta^{13}C$–0‰ could be an enriched in ^{13}C source, at least at the urban site. It has been shown that $CaCO_3$ desorbs from filter samples in He at temperatures >550 °C (Huang et al., 2006). Even though we did not expect much carbonate carbon in the PM_1 fraction, we cannot exclude that small amounts are present in some samples. Due to the strong difference in $\delta^{13}C$ between carbonate carbon and OC, even a small amount (up to 15%) would be sufficient to significantly alter $\delta^{13}C_{OC,650}$.

We tested the desorption of $CaCO_3$, using small amounts of $CaCO_3$ standard material applied to pre-cleaned filters. We found that $CaCO_3$ desorbed at 650 °C, but did not desorb at 550 °C. Therefore we re-analyzed the urban filter samples with a reduced desorption temperature of 550 °C for the third temperature step. We found that OC desorbed at 550 °C had in most cases significantly depleted $\delta^{13}C_{OC,550}$ values compared to OC desorbed at 650 °C and that $\delta^{13}C_{OC,550}$ was more comparable to $\delta^{13}C_{OC}$ values measured at the lower temperature steps (200 °C and 350 °C). For the coastal and forest site $\delta^{13}C_{OC}$ was the same for desorption temperatures of 550 °C and 650 °C within experimental uncertainties.

In addition, we tried to directly remove carbonates by acidification for samples from the urban, coastal and forest site, even though $CaCO_3$ is not an expected major source in PM_1 at the forest and coastal sites. After carbonate removal, $\delta^{13}C$ values had almost the same values as before

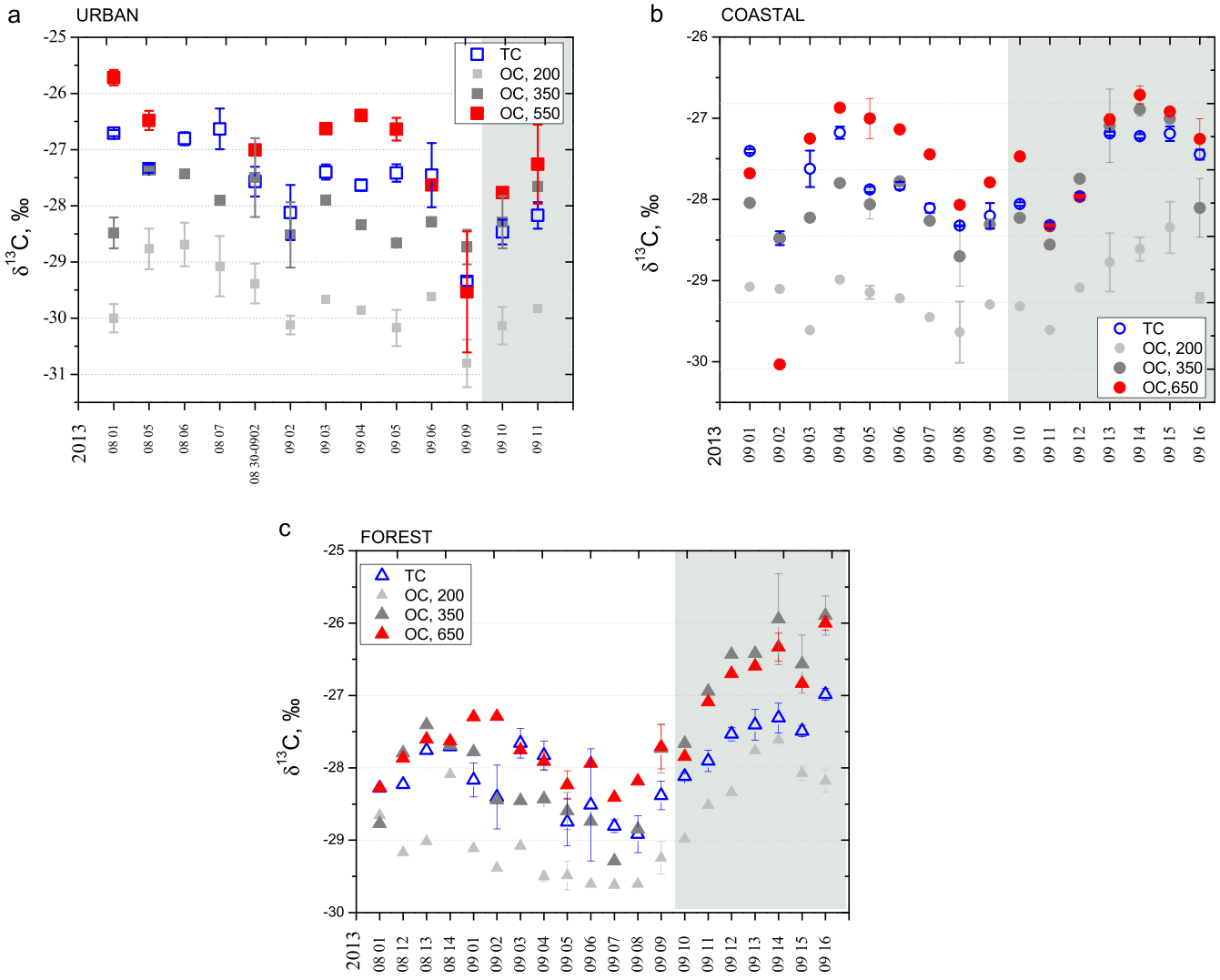

Figure 3. $\delta^{13}C_{TC}$ and $\delta^{13}C_{OC}$ at all three sites over the whole measurement period. The shading area denotes a polluted episode from 10 to 17 September. $\delta^{13}C_{OC}$ was measured at different desorption temperatures and the denoted number (200, 350, 550, 650) gives the respective temperature. Error bars denote the standard deviation, if repeated measurements were made, data points without error bars were measured only once.

carbonate removal for the 200 °C and 350 °C temperature steps. However, at the 650 °C step obvious artifacts were caused by the acid treatment (increased instead of decreased OC mass and unrealistically depleted $\delta^{13}C_{OC,650}$ values down to −42‰). This indicates that the acid treatment cannot be used for our purpose (figure A1-A3 in the supporting material). Therefore we kept 550 °C as the highest temperature step for the urban site and used 650 °C data for the other two sites.

The isotopic composition of organic carbon measured at different temperature steps is presented in Fig. 3(a and b, c). $\delta^{13}C_{OC}$ follows a similar temporal trend as $\delta^{13}C_{TC}$ at all three sites. All $\delta^{13}C_{OC,200}$ values are depleted compared to $\delta^{13}C_{TC}$ values. The depletion was observed for all values for all three sites. In principle this could be an artefact of the thermal desorption process, but based on tests (Dusek et al., 2013a; Zenker et al., 2020) this effect is expected to be rather small. It is more likely that this depletion is due to (biogenic) SOA, which is depleted with respect to the precursor gases, if they are only partially reacted (Irei et al., 2014). Additionally measurements of biogenic SOA precursor gases have shown that they have relatively depleted $\delta^{13}C$ signatures (Haberstroh et al., 2019), but this could vary with tree species and even environmental conditions (Rudolph et al., 2003), and photochemical aging could modify the original SOA signature. That OC desorbed at 200 °C falls into the range of published values of SOA precursors, is therefore not 100% conclusive evidence that this OC fraction is due to biogenic SOA.

The values of OC desorbed at 350 °C are close to TC values for most days. The difference from TC is on average 0.5‰, 0.2‰ and 0.1‰ in urban, coastal and forest sites respectively. However, $\delta^{13}C_{OC,\ 350}$ values were depleted compared to $\delta^{13}C_{TC}$ values during the clean period and enriched during the polluted period at the coastal and urban site. The largest variation of $\delta^{13}C_{OC}$ values is observed at the highest desorption temperature (650 °C, and 550 °C for the urban site). Nearly all OC, 550 and/or OC, 650 values are enriched compared to TC (with the urban values showing the highest differences), and mostly, they have the highest values of all components, but in the polluted episode the OC, 350 values are close to TC. The difference of isotopic composition of organic carbon at 650 °C and stable carbon isotope values of total carbon ($\delta^{13}C_{OC,650}$- $\delta^{13}C_{TC}$) varied from −0.3 to 0.9‰ at the coastal site and from −0.5 to 0.6‰ at the forest site. The highest difference was found at the urban site where $\delta^{13}C_{OC,550}$ - $\delta^{13}C_{TC}$ varied from −0.2 to 1.2‰. In the pollution episode, air masses originated from south, southeast or southwest direction indicating long-range transport of pollutants from Eastern Europe and Southern Europe to Lithuania. Zhang et al. (2019) demonstrated that $\delta^{13}C$ values of water soluble organic carbon, which may compose up to 75% of OC, increases during long-range transport. Oxidative processing during long-range transport or the different source could cause the enrichment of $\delta^{13}C_{OC}$ values during the polluted episode (Aggarwal and Kawamura, 2008; Wang et al., 2010; Wang and Kawamura, 2006).

3.2. Clean and polluted episodes

A comparison between sites revealed a similar pattern at forest and coastal sites, where $\delta^{13}C$ values in the clean period were more variable and clearly more depleted at the forest site. Here data from September month only is presented when the measurements were performed at both sites simultaneously. The polluted period (09 10–09 16) is characterized by a gradual enrichment in $\delta^{13}C$ compared to the clean period (09 01–09 09). At the coastal and forest sites $\delta^{13}C$ was enriched during polluted episodes compared to clean episodes at all OC desorption temperature steps (200, 350 and 650 °C) (Fig. 4(a and b)). The highest difference between the two distinct episodes occurred at the forest site where the difference was up to 2‰ (Fig. 4 (b)). For the urban site, only two filters were available during the polluted period, preventing a sound comparison between clean and polluted periods.

The isotopic composition of OC depends on the isotopic composition of the major sources and potentially also on chemical processes that OC undergoes in the atmosphere. Therefore, $\delta^{13}C$ of OC can be influenced by meteorological conditions (humidity, temperature, solar radiation) as they can change the chemical processes that act on the organic aerosol and/or by wind direction, which can indicate different source contributions depending on air mass origin. Despite the low number of observations some dependence of $\delta^{13}C$ on sunshine hours and wind direction was observed at the forest site. For the urban site no clear dependence of $\delta^{13}C_{OC}$ on meteorological parameters was observed, likely due to the proximity and variability of primary emission sources in the urban environment. At the coastal site there was also no clear dependency of $\delta^{13}C_{OC}$ versus meteorological conditions (Fig. A4-A5 in the supporting material). Fig. 5(a and b, c) shows the dependence of $\delta^{13}C_{OC}$ at three different desorption temperatures on sun shine hours and wind direction at the forest site. Fig. 5 (a) presents sun shine hours via $\delta^{13}C_{OC,200}$ for two different wind sectors (west and north in blue and east in red). The $\delta^{13}C_{OC,200}$ values are clearly different for the different wind sectors, with the easterly wind sector showing enriched ^{13}C signatures compared to the westerly wind sector, especially for low sunshine. A weaker dependence was observed between $\delta^{13}C_{OC,200}$ and sun shine hours. Longer sunshine hours are an indicator of enhanced photochemical activity, most likely resulting in stronger SOA formation locally at the forest site. However, local sunshine hours are not a perfect indicator of photochemical aging, as that process of course depends on the sunshine hours along the whole back trajectory. During westerly and north wind direction $\delta^{13}C_{OC,200}$ (blue symbols) did not depend on sunshine hours ($R^2 = 0.2$) and are close to published values of α-pinene, a SOA precursor. Our hypothesis is that during westerly and north wind directions relatively clean air masses reach the site without much long-range transport of anthropogenic pollution. OA should then be dominated by local/regional biogenic SOA formation, irrespective of local sunshine hours. On the other hand an anti-correlation ($R^2 = 0.5$) between sunshine hours and $\delta^{13}C_{OC,200}$ was observed during easterly wind direction (red symbols), such that $\delta^{13}C_{OC}$ values tend to be enriched for low sunshine hours and become more depleted with longer sunshine hours. During south-easterly wind directions air masses are advected over more polluted regions and we assume that OC results from local production of SOA (which is depleted in ^{13}C) that condenses on OA transported to the site. Higher temperature and high solar radiation are associated with increased SOA formation. On days with longer sunshine hours the regional SOA formation presumably dominates over long-range transport and $\delta^{13}C_{OC,200}$ values approach the ones measured during the clean conditions north and westerly wind directions. If there are only few sun hours (little solar radiation) local SOA formation is weak and the total OA $\delta^{13}C$ values are dominated by the relatively enriched values associated with long-range transport. This hypothesis still requires further corroboration, for example by analysing chemical SOA tracers, or laboratory experiments into SOA formation and aging. $\delta^{13}C_{OC}$ measured at 350 °C ($R^2 = 0.3$) and 650 °C ($R^2 = 0.5$) showed potentially a slight tendency towards depleted values (Fig. 5(b and c)), when solar radiation was high, but there are too few data points for a firm conclusion.

Fig. 5(d) shows the difference between more and less volatile fractions of organic carbon expressed as $\delta^{13}C_{OC,350}$ - $\delta^{13}C_{OC,650}$ (‰). As suggested in Masalaite (2017), this difference can be indicative of photochemical aging, since more oxidized and less volatile reaction products tend to accumulate in the less volatile OC fraction. Due to the kinetic isotope effect these reaction products tend to be depleted in ^{13}C. Indeed, during easterly wind directions (associated with longer aging times during long-range transport) the less volatile fraction (OC, 650) was depleted in ^{13}C compared to the more volatile fraction (OC, 350). However, for westerly and north wind directions this effect is absent, as would be expected, if the aerosol is more locally produced and less aged (in fact OC, 350 is slightly depleted compared to OC, 650).

Fig. 6 shows the OC mass concentration desorbed at different temperature steps (thermogram) for each site during clean and polluted episodes. The desorbed total OC mass concentration was clearly the

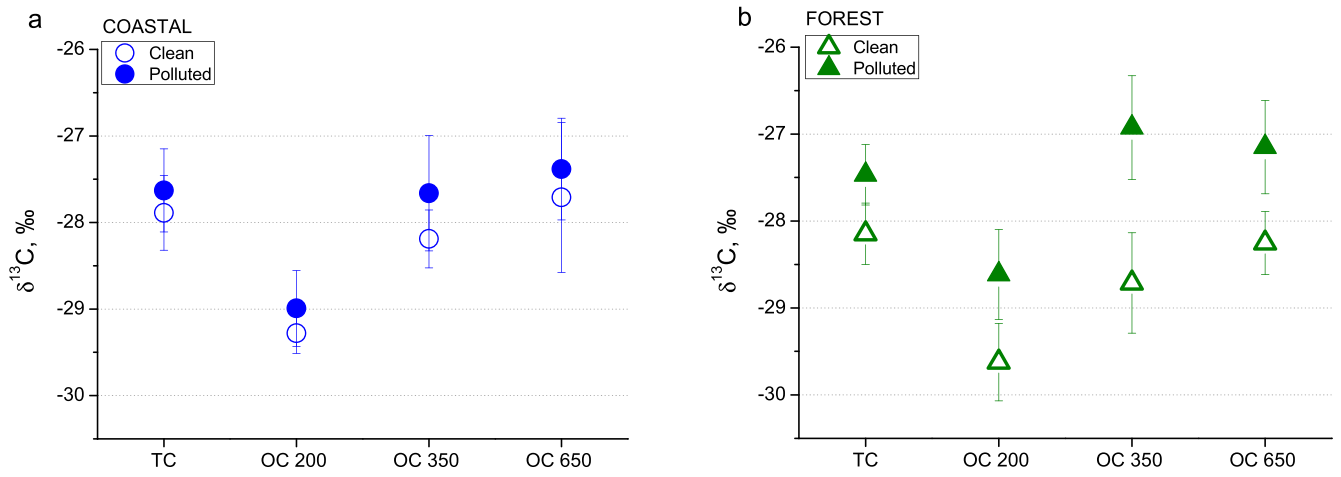

Figure 4. $\delta^{13}C$ variation of ambient aerosol samples collected at the coastal and forest sites at different desorption temperature: 200 °C, 350 °C and 650 °C during clean and polluted episodes. Error bars indicate standard deviation over clean and polluted measurement periods, respectively.

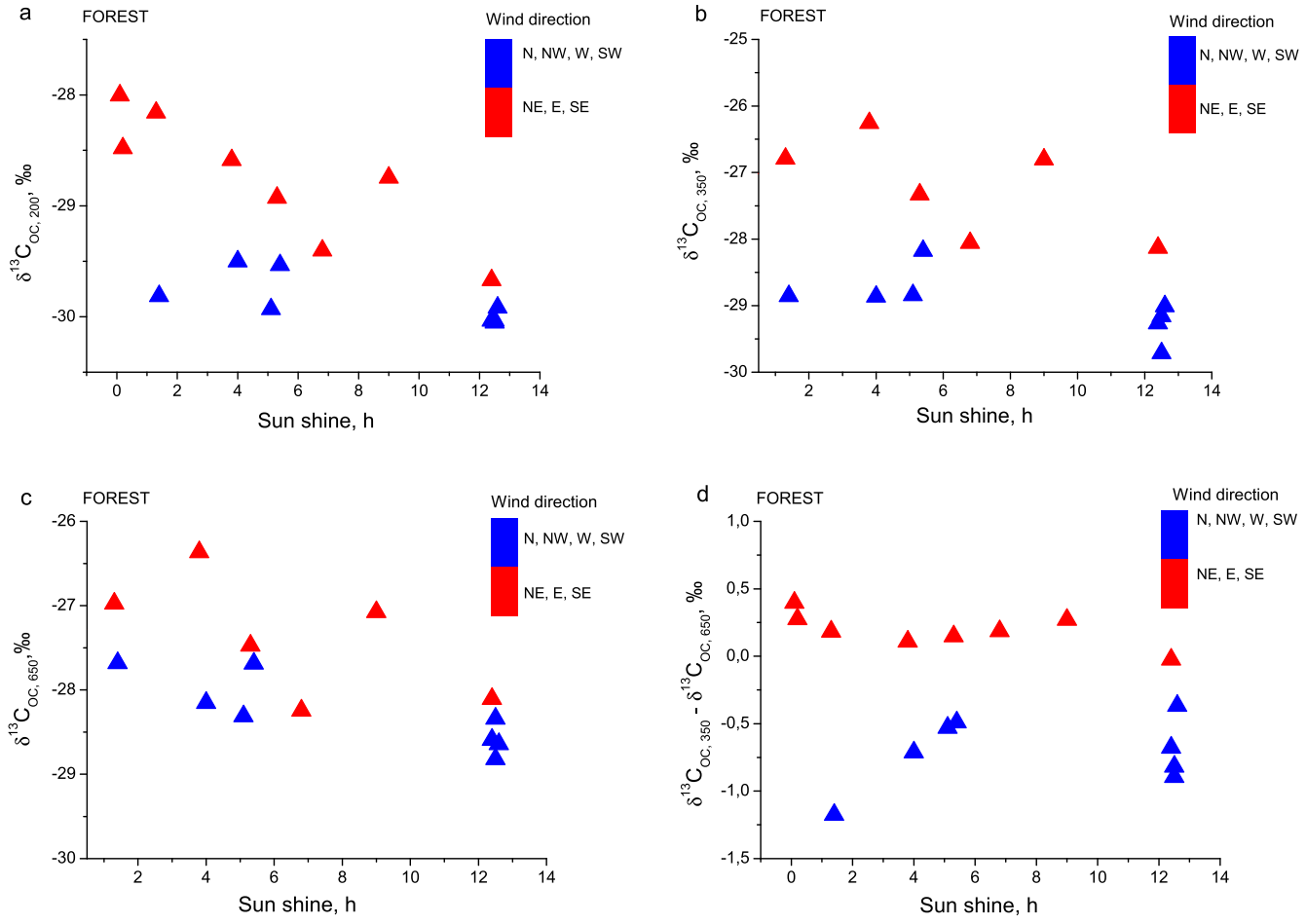

Figure 5. $\delta^{13}C_{OC}$ dependence on sun shine hours and dominant wind direction at forest site.

highest at the urban site (5.04 μg/m^3) during the polluted episode and smallest at the forest site (1.09 μg/m^3) during the clean episode. OC desorbed at 350 °C accounted for the highest fraction of OC mass fraction at all sites, both during polluted and clean periods. More refractory OC released at the 650 °C temperature step constitutes ~30% of total OC at all sites.

3.3. Comparison with winter-time data

A previous study analyzed $\delta^{13}C$ of carbonaceous aerosol samples (PM_1 fraction) collected at the same three sites (urban, coastal and forest) in winter (Masalaite et al., 2017). Carbonaceous aerosol was clearly depleted in ^{13}C in summer samples compared to the winter samples, both for total carbon (Fig. 7) and OC desorbed at different temperature steps (Fig. 8 (a)). In winter $\delta^{13}C$ of TC and OC varied

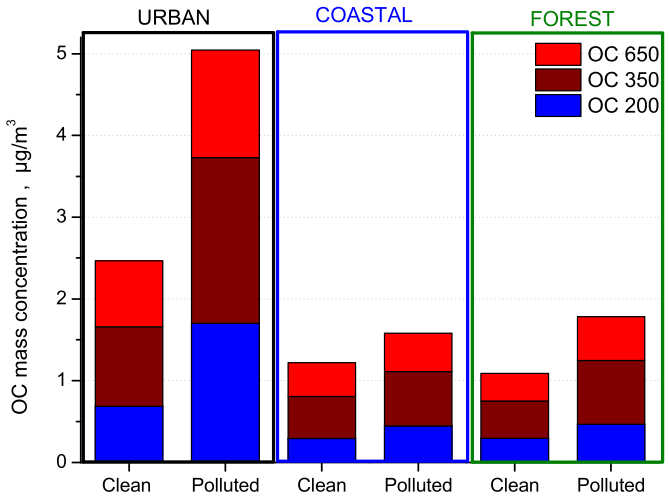

Fig. 6. Desorbed Organic Carbon (OC) mass concentration at different desorption temperatures: 200 °C, 350 °C and 650 °C (550 °C at the urban site) during clean and polluted episodes at the three sites.

between gasoline/diesel fuel combustion generated particles typical for Eastern Europe (−28 ± 0.9‰) and particles emitted from a source with $\delta^{13}C_{TC} = -25.1 \pm 0.2$‰ (i.e. biomass burning emissions or a mixture of biomass and coal burning). Comparing with our present data, the seasonal difference is evident at all sites and can be most clearly seen for the forest site (Fig. 7). Note that we used the measured $\delta^{13}C$ values for the urban site without removal of the carbonates for the seasonal comparison, since the carbonates were not removed in the previous winter samples study.

The observed difference in isotopic composition is primarily due to different pollution sources during summer and winter. Biomass burning is still widely used for domestic heating in Lithuania and it is one of the dominant sources of aerosol particles in winter (Masalaite et al., 2017). The main types of biomass used for heating in the winter-time have a relatively enriched isotopic signature ranging from −25.5‰ to −27.0‰ (Garbaras et al., 2015) and particles from coal combustion have $\delta^{13}C$ of around −25 ± 0.5‰ (Widory, 2006). $\delta^{13}C_{TC}$ values at the forest site were the most enriched in ^{13}C compared to the average $\delta^{13}C_{TC}$ of all three sites in winter time, most likely due to less traffic sources in the area. However, in the summer, isotopic signatures at all three sites are

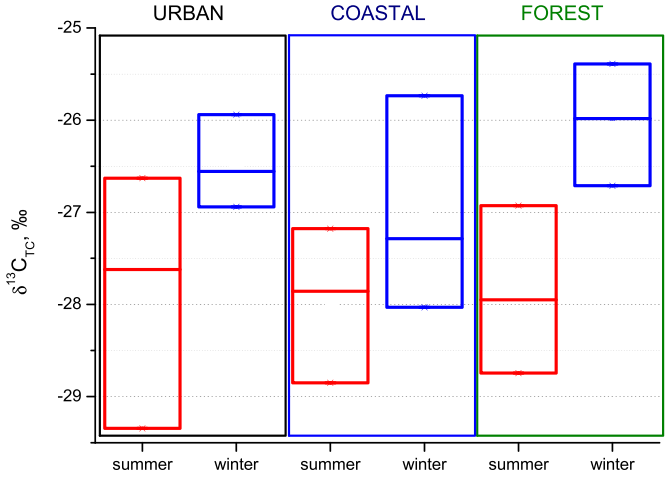

Figure 7. $\delta^{13}C_{TC}$ variation in summer and winter seasons at all three sites. The minimum and maximum values are the end and beginning of the box, meanwhile the average value is represented as a line in the middle of the box. The summer values are from this study, the winter values are from Masalaite et al. (2017).

comparable. A strong reduction in biomass burning in the summer is therefore a likely cause of the depleted ^{13}C signatures for both TC and OC. Only particles released during gasoline and diesel combustion are common all year round and independent of the season. This source of aerosol particles may be dominant in the urban area during summer time when all sources of heating (coal, biomass burning and so on) are absent.

On the other hand, the summer time is favorable for biogenic emissions and enhanced secondary organic aerosol formation from biogenic or anthropogenic sources. The isotopic signature of ambient biogenic SOA is not very well known, as in most chamber experiments commercially available SOA precursors are used for experiments. Studies by Fisseha et al. (2009b) and Haberstroh et al. (2019) provides evidence that biogenic SOA precursors are depleted compared to bulk plant biomass due to the way in which they are metabolized. So we can assume that BSOA precursors are depleted and SOA formation itself leads to even more depleted aerosol products, if the precursor is only partially reacted. However, the $\delta^{13}C$ of the primary biogenic aerosol can be assumed to be in the same range as BB (−28 to − 26‰). Our $\delta^{13}C$ measurements of OC during the clean period at the forest site might be a good approximation of the isotopic signature of biogenic SOA in a pine tree dominated forest. The relatively depleted isotopic $\delta^{13}C_{OC}$ values of around −29‰ (OC, 200) (see Fig. 2) are in line with the $\delta^{13}C$ values of β-pinene reported by Fisseha et al. (2009b) and α-pinene reported by Haberstroh et al. (2019). An increase of biogenic SOA during summer time would further contribute to depleted 13C signatures of the organic aerosol compared to winter time.

$\delta^{13}C_{OC}$ values at different desorption temperatures were also depleted in summer samples compared to winter samples (Fig. 8 (a)), in the same way as with $\delta^{13}C_{TC}$ values. Note that we used the measured $\delta^{13}C_{OC}$ values in two desorption temperature ranges (100–200 °C and 250–350 °C) for the seasonal comparison, since this was the maximum desorption temperature in the previous winter study. In the summer, $\delta^{13}C_{OC}$ values were similar at all sites and at the three desorption temperature steps (Fig. 4), whereas in the winter $\delta^{13}C_{OC}$ values were the most enriched in the urban site and more depleted at coastal and forest site. This difference between the sites in winter was explained by SOA formation (which leads to OC depleted in ^{13}C). SOA formation is slow in winter. Therefore, primary aerosol particles prevail at the urban sites and increased contribution of SOA is apparent at the more remote sites. In the summer, SOA formation is important at all three sites, leading to OC that is depleted with respect to TC.

This is also supported by a large difference in $\delta^{13}C$ between more and less refractory OC, found in this study for the summer. This large difference can be related to a higher contribution of secondary organic compounds (biogenic and other). SOA is thought to be isotopically depleted due to kinetic fractionation and likely depleted biogenic precursor gases. Since recently formed SOA tends to contribute significantly to the less refractory OC, this results in a OC, 200 that is depleted compared to OC, 350. In winter the difference between OC desorbed at lower and higher temperatures (less and more refractory OC) is small at the urban site (Masalaite et al., 2017), which is typical for primary sources (Zenker et al., 2020) and it becomes larger for the coastal and forest sites.

Despite the importance of SOA formation, in summer the aerosol contains a higher fraction of more refractory OC than in winter at all three sites (Fig. 8(b)). The difference was highest at the urban site - from 70% of less refractory OC in winter to 70% of more refractory OC in summer. There are several possible reasons for such change. First, partitioning of semi-volatile OC to the particle phase is reduced in summer due to the higher ambient temperatures. This would lead to a lower fraction of OC that is desorbed at the 200 °C temperature step (Ma et al., 2016; Ni et al., 2019). However, this cannot explain the difference between the sites, since temperatures were warmer in summer at all three sites. A higher fraction of more refractory OC (Fig. 8 (b)) can also suggest active photochemical processing of the primary organic aerosol and/or

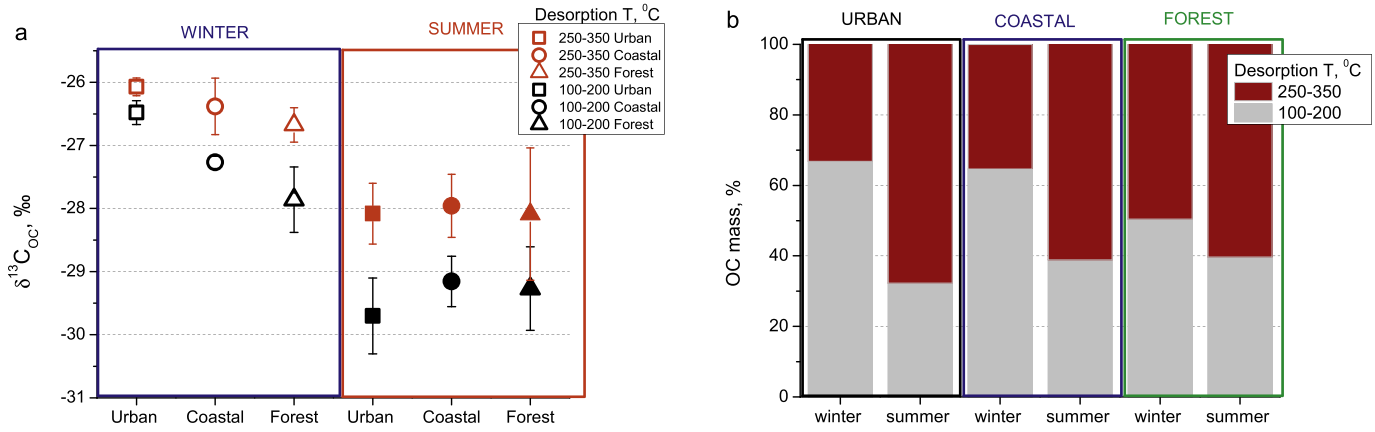

Fig. 8. Comparison of $\delta^{13}C_{OC}$–thermograms of ambient aerosol samples collected at the urban, coastal and forest sites during winter and summer time; error bars corresponds to the standard deviation of monthly averaged value (a) and fraction of OC at two desorption temperatures (b) Summer data are from this study, winter data from Masalaite et al. (2017).

SOA. Photochemical processing is enhanced in the summer and is known to make the aerosol less volatile (Holzinger et al., 2013; Kroll and Seinfeld, 2008). Primary OC is usually much more volatile than aged, ambient particles (Keller and Burtscher, 2017; Vodička et al., 2015). This is in line with our previous hypothesis that at the urban site OC is mostly primary in winter and suggests that photochemical processing changes OC properties at the urban scale in summer. In principle, photochemical processing would lead to an enriched ^{13}C signature in the less refractory OC, via the kinetic isotope effect. Since the ^{13}C signature of the original (biogenic) SOA is unknown, it is unclear if and to which extent this effect is important.

4. Conclusions

The stable carbon isotope variation of carbonaceous aerosol was investigated at three different sites (urban, coastal and forest) in Lithuania during August and September 2013. The collected samples showed a similar isotopic composition for TC as well as for OC at all three sites. The most depleted $\delta^{13}C$ values were found during a clean episode, with air masses from the North Atlantic Ocean, the Norwegian Sea and Northern Europe. In contrast, $\delta^{13}C$ values were enriched at all OC desorption temperature steps during a polluted episode, where long-range transport of air masses from Eastern Europe and Southern Europe prevailed. From the start to the end of the pollution episode the $\delta^{13}C_{OC}$ values increased by 2‰ on average. Our study suggests that of all the many potential sources contributing to the carbonaceous matter, increased biogenic SOA formation during the sunny days of the pollution episode most likely explains this observation. Long aging time of the organic aerosol during long-range transport, which can change $\delta^{13}C_{OC}$ via kinetic fractionation, could explain depleted $\delta^{13}C$ values in the most refractory OC fraction in the polluted episode.

The seasonal comparison of the isotopic composition measured at all three sites (by combining data from this study with a prior one (Masalaite et al., 2017) revealed that carbonaceous aerosol was clearly enriched in ^{13}C in winter samples compared to summer samples. The seasonal difference is evident at all sites and reflects the absence of biomass burning emissions in summer, which are isotopically enriched compared to liquid fossil fuel burning emissions. The effect can be most clearly seen at the forest site.

The differences in $\delta^{13}C$ between more and less refractory OC is larger during summer time, which can be explained by stronger photochemical aerosol aging and/or SOA formation. An analysis at different desorption temperatures revealed that refractiveness of the aerosol particles changes during the seasons. Less refractory OC, desorbed at temperatures below 200 °C was dominant during winter time at all three sites, whereas more refractory OC dominated during summer time. A larger fraction of more volatile OC could be caused by partitioning of semi-volatile OC to the particle phase due to the lower ambient temperatures in winter. In addition, photochemical processing makes the aerosol less volatile and these processes are enhanced in the summer. Considering the fact that primary OC is more volatile than aged, ambient particles, we can conclude that OC is mostly primary in winter (biomass burning) at the urban site, whereas in summer photochemical processing is active which thus changes OC properties at the urban scale.

Author contributions section

Agne Masalaite: Conceptualization, Formal analysis, Investigation, Writing - Original Draft.

Vidmantas Remeikis: Resources, Supervision, Project administration.

Katrin Zenker: Investigation, Data Curation.

Iris Westra: Investigation.

Harro Meijer: Resources, Writing - Review & Editing.

Ulrike Dusek: Conceptualization, Methodology, Resources, Writing - Review & Editing.

Declaration of competing interest

The authors declare that they have no known competing financial interests or personal relationships that could have appeared to influence the work reported in this paper.

Acknowledgements

This study was funded by the Research Council of Lithuania (Grant No. P-KEL-17-38).

Appendix A. Supplementary data

Supplementary data to this article can be found online at https://doi.org/10.1016/j.atmosenv.2020.117374.

References

Aggarwal, S.G., Kawamura, K., 2008. Molecular distributions and stable carbon isotopic compositions of dicarboxylic acids and related compounds in aerosols from Sapporo, Japan: implications for photochemical aging during long-range atmospheric transport. J. Geophys. Res.: Atmosphere 113.

Aggarwal, S., Kawamura, K., Umarji, G., Tachibana, E., Patil, R., Gupta, P., 2013. Organic and inorganic markers and stable C-, N-isotopic compositions of tropical coastal aerosols from megacity Mumbai: sources of organic aerosols and atmospheric processing. Atmos. Chem. Phys. 13, 4667–4680.

Ballentine, D.C., Macko, S.A., Turekian, V.C., 1998. Variability of stable carbon isotopic compositions in individual fatty acids from combustion of C4 and C3 plants: implications for biomass burning. Chem. Geol. 152, 151–161.
Bond, T.C., Bhardwaj, E., Dong, R., Jogani, R., Jung, S., Roden, C., Streets, D.G., Trautmann, N.M., 2007. Historical emissions of black and organic carbon aerosol from energy-related combustion, 1850–2000. Global Biogeochem. Cycles 21.
Butt, E., Rap, A., Schmidt, A., Scott, C., Pringle, K., Reddington, C., Richards, N., Woodhouse, M., Ramirez-Villegas, J., Yang, H., 2016. The impact of residential combustion emissions on atmospheric aerosol, human health, and climate. Atmos. Chem. Phys. 16, 873–905.
Cao, J.-j., Chow, J.C., Tao, J., Lee, S.-c., Watson, J.G., Ho, K.-f., Wang, G.-h., Zhu, C.-s., Han, Y.-m., 2011. Stable carbon isotopes in aerosols from Chinese cities: influence of fossil fuels. Atmos. Environ. 45, 1359–1363.
Ceburnis, D., Masalaite, A., Ovadnevaite, J., Garbaras, A., Remeikis, V., Maenhaut, W., Claeys, M., Sciare, J., Baisnée, D., O'Dowd, C.D., 2016. Stable isotopes measurements reveal dual carbon pools contributing to organic matter enrichment in marine aerosol. Sci. Rep. 6, 36675.
Chesselet, R., Fontugne, M., Buat-Ménard, P., Ezat, U., Lambert, C., 1981. The origin of particulate organic carbon in the marine atmosphere as indicated by its stable carbon isotopic composition. Geophys. Res. Lett. 8, 345–348.
Crippa, M., DeCarlo, P., Slowik, J., Mohr, C., Heringa, M., Chirico, R., Poulain, L., Freutel, F., Sciare, J., Cozic, J., 2013. Wintertime aerosol chemical composition and source apportionment of the organic fraction in the metropolitan area of Paris. Atmos. Chem. Phys. 13, 961–981.
Dusek, U., Meusinger, C., Oyama, B., Ramon, W., de Wilde, P., Holzinger, R., Röckmann, T., 2013a. A thermal desorption system for measuring δ13C ratios on organic aerosol. J. Aerosol Sci. 66, 72–82.
Dusek, U., Ten Brink, H., Meijer, H., Kos, G., Mrozek, D., Röckmann, T., Holzinger, R., Weijers, E., 2013b. The contribution of fossil sources to the organic aerosol in The Netherlands. Atmos. Environ. 74, 169–176.
Dusek, U., Hitzenberger, R., Kasper-Giebl, A., Kistler, M., Meijer, H.A., Szidat, S., Wacker, L., Holzinger, R., Röckmann, T., 2017. Sources and formation mechanisms of carbonaceous aerosol at a regional background site in The Netherlands: insights from a year-long radiocarbon study. Atmos. Chem. Phys. 17, 3233–3251.
Fisseha, R., Saurer, M., Jäggi, M., Siegwolf, R.T., Dommen, J., Szidat, S., Samburova, V., Baltensperger, U., 2009a. Determination of primary and secondary sources of organic acids and carbonaceous aerosols using stable carbon isotopes. Atmos. Environ. 43, 431–437.
Fisseha, R., Spahn, H., Wegener, R., Hohaus, T., Brasse, G., Wissel, H., Tillmann, R., Wahner, A., Koppmann, R., Kiendler-Scharr, A., 2009b. Stable carbon isotope composition of secondary organic aerosol from β-pinene oxidation. J. Geophys. Res.: Atmosphere 114.
Garbaras, A., Masalaite, A., Garbariene, I., Ceburnis, D., Krugly, E., Remeikis, V., Puida, E., Kvietkus, K., Martuzevicius, D., 2015. Stable carbon fractionation in size-segregated aerosol particles produced by controlled biomass burning. J. Aerosol Sci. 79, 86–96.
Garbaras, A., Šapolaitė, J., Garbarienė, I., Ežerinskis, Ž., Mašalaitė-Nalivaikė, A., Skipitytė, R., Plukis, A., Remeikis, V., 2018. Aerosol source (biomass, traffic and coal emission) apportionment in Lithuania using stable carbon and radiocarbon analysis. Isot. Environ. Health Stud. 54, 463–474.
Garbarienė, I., Šapolaitė, J., Garbaras, A., Ežerinskis, Ž., Pocevičius, M., Krikščikas, L., Plukis, A., Remeikis, V., 2016. Origin identification of carbonaceous aerosol particles by carbon isotope ratio analysis. Aerosol Air Qual. Res. 16, 1356–1365.
Górka, M., Rybicki, M., Simoneit, B.R., Marynowski, L., 2014. Determination of multiple organic matter sources in aerosol PM10 from Wrocław, Poland using molecular and stable carbon isotope compositions. Atmos. Environ. 89, 739–748.
Haberstroh, S., Kreuzwieser, J., Boeddeker, H., Eiblmeier, M., Gutte, H., Lobo-do-Vale, R., Caldeira, M.C., Werner, C., 2019. Natural carbon isotope composition distinguishes compound groups of biogenic volatile organic compounds (BVOC) in two Mediterranean woody species. Front. For. Glob. Change 2, 55.
Hallquist, M., Wenger, J.C., Baltensperger, U., Rudich, Y., Simpson, D., Claeys, M., Dommen, J., Donahue, N., George, C., Goldstein, A., 2009. The formation, properties and impact of secondary organic aerosol: current and emerging issues. Atmos. Chem. Phys. 9, 5155–5236.
Holzinger, R., Goldstein, A., Hayes, P., Jimenez, J., Timkovsky, J., 2013. Chemical evolution of organic aerosol in Los Angeles during the CalNex 2010 study. Atmos. Chem. Phys. 13, 10125–10141.
Huang, L., Brook, J., Zhang, W., Li, S., Graham, L., Ernst, D., Chivulescu, A., Lu, G., 2006. Stable isotope measurements of carbon fractions (OC/EC) in airborne particulate: a new dimension for source characterization and apportionment. Atmos. Environ. 40, 2690–2705.
Irei, S., Takami, A., Hayashi, M., Sadanaga, Y., Hara, K., Kaneyasu, N., Sato, K., Arakaki, T., Hatakeyama, S., Bandow, H., 2014. Transboundary secondary organic aerosol in western Japan indicated by the δ13C of water-soluble organic carbon and the m/z 44 signal in organic aerosol mass spectra. Environ. Sci. Technol. 48, 6273–6281.
Jacobson, M., Hansson, H.C., Noone, K., Charlson, R., 2000. Organic atmospheric aerosols: review and state of the science. Rev. Geophys. 38, 267–294.
Jimenez, J.L., Canagaratna, M., Donahue, N., Prevot, A., Zhang, Q., Kroll, J.H., DeCarlo, P.F., Allan, J.D., Coe, H., Ng, N., 2009. Evolution of organic aerosols in the atmosphere. Science 326, 1525–1529.
Kawamura, K., Kobayashi, M., Tsubonuma, N., Mochida, M., Watanabe, T., Lee, M., 2004. Organic and Inorganic Compositions of Marine Aerosols from East Asia: Seasonal Variations of Water-Soluble Dicarboxylic Acids, Major Ions, Total Carbon and Nitrogen, and Stable C and N Isotopic Composition. The Geochemical Society Special Publications. Elsevier, pp. 243–265.
Keller, A., Burtscher, H., 2017. Characterizing particulate emissions from wood burning appliances including secondary organic aerosol formation potential. J. Aerosol Sci. 114, 21–30.
Kirillova, E.N., Sheesley, R.J., Andersson, A., Gustafsson, O., 2010. Natural abundance 13C and 14C analysis of water-soluble organic carbon in atmospheric aerosols. Anal. Chem. 82, 7973–7978.
Kroll, J.H., Seinfeld, J.H., 2008. Chemistry of secondary organic aerosol: formation and evolution of low-volatility organics in the atmosphere. Atmos. Environ. 42, 3593–3624.
Kundu, S., Kawamura, K., Andreae, T.W., Hoffer, A., Andreae, M.O., 2010. Diurnal variation in the water-soluble inorganic ions, organic carbon and isotopic compositions of total carbon and nitrogen in biomass burning aerosols from the LBA-SMOCC campaign in Rondônia, Brazil. J. Aerosol Sci. 41, 118–133.
Ma, J., Li, X., Gu, P., Dallmann, T.R., Presto, A.A., Donahue, N.M., 2016. Estimating ambient particulate organic carbon concentrations and partitioning using thermal optical measurements and the volatility basis set. Aerosol. Sci. Technol. 50, 638–651.
Martinsson, J., Andersson, A., Sporre, M.K., Friberg, J., Kristensson, A., Swietlicki, E., Olsson, P.-A., Stenström, K.E., 2017. Evaluation of δ13C in carbonaceous aerosol source apportionment at a rural measurement site. Aerosol Air Qual. Res. 17, 2081–2094.
Masalaite, A., Remeikis, V., Garbaras, A., Dudoitis, V., Ulevicius, V., Ceburnis, D., 2015. Elucidating carbonaceous aerosol sources by the stable carbon δ13CTC ratio in size-segregated particles. Atmos. Res. 158, 1–12.
Masalaite, A., Holzinger, R., Remeikis, V., Roeckmann, T., Dusek, U., 2017. Characteristics, sources and evolution of fine aerosol (PM1) at urban, coastal and forest background sites in Lithuania. Atmos. Environ. 148, 62–76.
Masalaite, A., Garbaras, A., Remeikis, V., 2012. Stable isotopes in environmental investigations. Lith. J. Phys. 52, 261–268.
Masalaite, A., Holzinger, R., Ceburnis, D., Remeikis, V., Ulevičius, V., Röckmann, T., Dusek, U., 2018. Sources and atmospheric processing of size segregated aerosol particles revealed by stable carbon isotope ratios and chemical speciation. Environ. Pollut. 240, 286–296.
Meusinger, C., Dusek, U., King, S.M., Holzinger, R., Rosenørn, T., Sperlich, P., Julien, M., Remaud, G.S., Bilde, M., Röckmann, T., 2017. Chemical and isotopic composition of secondary organic aerosol generated by α-pinene ozonolysis. Atmos. Chem. Phys. 17, 6373–6391.
Miyazaki, Y., Fu, P., Kawamura, K., Mizoguchi, Y., Yamanoi, K., 2012. Seasonal variations of stable carbon isotopic composition and biogenic tracer compounds of water-soluble organic aerosols in a deciduous forest. Atmos. Chem. Phys. 12, 1367–1376.
Mkoma, S.L., Kawamura, K., Tachibana, E., Fu, P., 2014. Stable carbon and nitrogen isotopic compositions of tropical atmospheric aerosols: sources and contribution from burning of C3 and C4 plants to organic aerosols. Tellus B 66, 20176.
Ni, H., Huang, R.-J., Cao, J., Liu, W., Zhang, T., Wang, M., Meijer, H.A., Dusek, U., 2018. Source apportionment of carbonaceous aerosols in Xi'an, China: insights from a full year of measurements of radiocarbon and the stable isotope 13 C. Atmos. Chem. Phys. 18, 16363–16383.
Ni, H., Huang, R.-J., Cao, J., Dai, W., Zhou, J., Deng, H., Aerts-Bijma, A., Meijer, H.A., Dusek, U., 2019. High contributions of fossil sources to more volatile organic carbon. Geophysical Research Abstracts.
Ovadnevaitė, J., Kvietkus, K., Šakalys, J., 2007. Evaluation of the impact of long-range transport and aerosol concentration temporal variations at the eastern coast of the Baltic Sea. Environ. Monit. Assess. 132, 365–375.
Pan, Y., Tian, S., Liu, D., Fang, Y., Zhu, X., Gao, M., Wentworth, G.R., Michalski, G., Huang, X., Wang, Y., 2018. Source apportionment of aerosol ammonium in an ammonia-rich atmosphere: an isotopic study of summer clean and hazy days in urban Beijing. J. Geophys. Res.: Atmosphere 123, 5681–5689.
Pavuluri, C.M., Kawamura, K., Swaminathan, T., Tachibana, E., 2011. Stable carbon isotopic compositions of total carbon, dicarboxylic acids and glyoxylic acid in the tropical Indian aerosols: implications for sources and photochemical processing of organic aerosols. J. Geophys. Res.: Atmosphere 116.
Pirjola, L., Niemi, J.V., Saarikoski, S., Aurela, M., Enroth, J., Carbone, S., Saarnio, K., Kuuluvainen, H., Kousa, A., Rönkkö, T., 2017. Physical and chemical characterization of urban winter-time aerosols by mobile measurements in Helsinki, Finland. Atmos. Environ. 158, 60–75.
Pöschl, U., 2005. Atmospheric aerosols: composition, transformation, climate and health effects. Angew. Chem. Int. Ed. 44, 7520–7540.
Pöschl, U., Shiraiwa, M., 2015. Multiphase chemistry at the atmosphere–biosphere interface influencing climate and public health in the anthropocene. Chem. Rev. 115, 4440–4475.
Putaud, J.-P., Raes, F., Van Dingenen, R., Brüggemann, E., Facchini, M.-C., Decesari, S., Fuzzi, S., Gehrig, R., Hüglin, C., Laj, P., 2004. A European aerosol phenomenology—2: chemical characteristics of particulate matter at kerbside, urban, rural and background sites in Europe. Atmos. Environ. 38, 2579–2595.
Putaud, J.-P., Van Dingenen, R., Alastuey, A., Bauer, H., Birmili, W., Cyrys, J., Flentje, H., Fuzzi, S., Gehrig, R., Hansson, H.-C., 2010. A European aerosol phenomenology–3: physical and chemical characteristics of particulate matter from 60 rural, urban, and kerbside sites across Europe. Atmos. Environ. 44, 1308–1320.
Puxbaum, H., Caseiro, A., Sánchez-Ochoa, A., Kasper-Giebl, A., Claeys, M., Gelencsér, A., Legrand, M., Preunkert, S., Pio, C., 2007. Levoglucosan levels at background sites in Europe for assessing the impact of biomass combustion on the European aerosol background. J. Geophys. Res.: Atmosphere 112.
Rudolph, J., Anderson, R.v., Czapiewski, K., Czuba, E., Ernst, D., Gillespie, T., Huang, L., Rigby, C., Thompson, A., 2003. The stable carbon isotope ratio of biogenic emissions

of isoprene and the potential use of stable isotope ratio measurements to study photochemical processing of isoprene in the atmosphere. J. Atmos. Chem. 44, 39–55.
Sang, X.F., Gensch, I., Laumer, W., Kammer, B., Chan, C.Y., Engling, G., Wahner, A., Wissel, H., Kiendler-Scharr, A., 2012. Stable carbon isotope ratio analysis of anhydrosugars in biomass burning aerosol particles from source samples. Environ. Sci. Technol. 46, 3312–3318.
Schumacher, C., Pöhlker, C., Aalto, P., Hiltunen, V., Petäjä, T., Kulmala, M., Pöschl, U., Huffman, J., 2013. Seasonal cycles of fluorescent biological aerosol particles in boreal and semi-arid forests of Finland and Colorado. Atmos. Chem. Phys. 13, 11987–12001.
Schurman, M., Lee, T., Desyaterik, Y., Schichtel, B., Kreidenweis, S., Collett Jr., J., 2015a. Transport, biomass burning, and in-situ formation contribute to fine particle concentrations at a remote site near Grand Teton National Park. Atmos. Environ. 112, 257–268.
Schurman, M., Lee, T., Sun, Y., Schichtel, B., Kreidenweis, S., Collett Jr., J., 2015b. Investigating types and sources of organic aerosol in Rocky Mountain National Park using aerosol mass spectrometry. Atmos. Chem. Phys. 15, 737–752.
Shiraiwa, M., Li, Y., Tsimpidi, A.P., Karydis, V.A., Berkemeier, T., Pandis, S.N., Lelieveld, J., Koop, T., Pöschl, U., 2017. Global distribution of particle phase state in atmospheric secondary organic aerosols. Nat. Commun. 8, 15002.
Stein, A., Draxler, R.R., Rolph, G.D., Stunder, B.J., Cohen, M., Ngan, F., 2015. NOAA's HYSPLIT atmospheric transport and dispersion modeling system. Bull. Am. Meteorol. Soc. 96, 2059–2077.
Sun, Y., Wang, Z., Dong, H., Yang, T., Li, J., Pan, X., Chen, P., Jayne, J.T., 2012. Characterization of summer organic and inorganic aerosols in Beijing, China with an aerosol chemical speciation monitor. Atmos. Environ. 51, 250–259.
Sun, Y., Wang, Z., Du, W., Zhang, Q., Wang, Q., Fu, P., Pan, X., Li, J., Jayne, J., Worsnop, D., 2015. Long-term real-time measurements of aerosol particle composition in Beijing, China: seasonal variations, meteorological effects, and source analysis. Atmos. Chem. Phys. 15, 10149–10165.
Swietlicki, E., 1989. European Source Region Identification of Long Range Transported Ambient Aerosol Based on PIXE Analysis and Related Techniques. Department of nuclear physics.
Szidat, S., Jenk, T.M., Synal, H.A., Kalberer, M., Wacker, L., Hajdas, I., Kasper-Giebl, A., Baltensperger, U., 2006. Contributions of fossil fuel, biomass-burning, and biogenic emissions to carbonaceous aerosols in Zurich as traced by 14C. J. Geophys. Res.: Atmosphere 111.
Szidat, S., Ruff, M., Perron, N., Wacker, L., Synal, H.-A., Hallquist, M., Shannigrahi, A.S., Yttri, K.E., Dye, C., Simpson, D., 2009. Fossil and non-fossil sources of organic carbon (OC) and elemental carbon (EC) in Göteborg, Sweden. Atmos. Chem. Phys. 9, 1521–1535.
Theodosi, C., Tsagkaraki, M., Zarmpas, P., Grivas, G., Liakakou, E., Paraskevopoulou, D., Lianou, M., Gerasopoulos, E., Mihalopoulos, N., 2018. Multi-year chemical composition of the fine-aerosol fraction in Athens, Greece, with emphasis on the contribution of residential heating in wintertime. Atmos. Chem. Phys. 18, 14371–14391.
Viana, M., Pey, J., Querol, X., Alastuey, A., De Leeuw, F., Lükewille, A., 2014. Natural sources of atmospheric aerosols influencing air quality across Europe. Sci. Total Environ. 472, 825–833.
Vodička, P., Schwarz, J., Cusack, M., Ždímal, V., 2015. Detailed comparison of OC/EC aerosol at an urban and a rural Czech background site during summer and winter. Sci. Total Environ. 518, 424–433.
Vodička, P., Kawamura, K., Schwarz, J., Kunwar, B., Ždímal, V., 2019. Seasonal study of stable carbon and nitrogen isotopic composition in fine aerosols at a Central European rural background station. Atmos. Chem. Phys. 19, 3463–3479.
Wang, H., Kawamura, K., 2006. Stable carbon isotopic composition of low-molecular-weight dicarboxylic acids and ketoacids in remote marine aerosols. J. Geophys. Res.: Atmosphere 111.
Wang, G., Xie, M., Hu, S., Gao, S., Tachibana, E., Kawamura, K., 2010. Dicarboxylic acids, metals and isotopic compositions of C and N in atmospheric aerosols from inland China: implications for dust and coal burning emission and secondary aerosol formation. Atmos. Chem. Phys. 10, 6087–6096.
Widory, D., 2006. Combustibles, fuels and their combustion products: a view through carbon isotopes. Combust. Theor. Model. 10, 831–841.
Widory, D., Roy, S., Le Moullec, Y., Goupil, G., Cocherie, A., Guerrot, C., 2004. The origin of atmospheric particles in Paris: a view through carbon and lead isotopes. Atmos. Environ. 38, 953–961.
Zhang, Q., Jimenez, J.L., Canagaratna, M., Allan, J., Coe, H., Ulbrich, I., Alfarra, M., Takami, A., Middlebrook, A., Sun, Y., 2007. Ubiquity and dominance of oxygenated species in organic aerosols in anthropogenically-influenced Northern Hemisphere midlatitudes. Geophys. Res. Lett. 34.
Zhang, R., Jing, J., Tao, J., Hsu, S.-C., Wang, G., Cao, J., Lee, C.S.L., Zhu, L., Chen, Z., Zhao, Y., 2013. Chemical characterization and source apportionment of PM 2.5 in Beijing: seasonal perspective. Atmos. Chem. Phys. 13, 7053–7074.
Zenker, K., Sirignano, C., Riccio, A., Chianese, E., Calfapietra, C., Prati Vittoria, M., Masalaite, A., Remeikis, V., Mook, E., Meijer A.J., H., Dusek, U., 2020. δ13C signatures of organic aerosols: measurement method evaluation and application in a source study. J. Aerosol Sci. https://doi.org/10.1016/j.jaerosci.2020.105534. In press.
Zhang, T., Cao, J.-J., Chow, J.C., Shen, Z.-X., Ho, K.-F., Ho, S.S.H., Liu, S.-X., Han, Y.-M., Watson, J.G., Wang, G.-H., 2014. Characterization and seasonal variations of levoglucosan in fine particulate matter in Xi'an, China. J. Air Waste Manag. Assoc. 64, 1317–1327.
Zhang, Y.L., Kawamura, K., Cao, F., Lee, M., 2016. Stable carbon isotopic compositions of low-molecular-weight dicarboxylic acids, oxocarboxylic acids, α-dicarbonyls, and fatty acids: implications for atmospheric processing of organic aerosols. J. Geophys. Res.: Atmosphere 121, 3707–3717.
Zhang, J., Tong, L., Huang, Z., Zhang, H., He, M., Dai, X., Zheng, J., Xiao, H., 2018. Seasonal variation and size distributions of water-soluble inorganic ions and carbonaceous aerosols at a coastal site in Ningbo, China. Sci. Total Environ. 639, 793–803.
Zhang, W., Zhang, Y.-L., Cao, F., Xiang, Y., Zhang, Y., Bao, M., Liu, X., Lin, Y.-C., 2019. High time-resolved measurement of stable carbon isotope composition in water-soluble organic aerosols: method optimization and a case study during winter haze in eastern China. Atmos. Chem. Phys. 19, 11071–11087.
Zielonka, U., Hlawiczka, S., Fudala, J., Wängberg, I., Munthe, J., 2005. Seasonal mercury concentrations measured in rural air in Southern Poland: contribution from local and regional coal combustion. Atmos. Environ. 39, 7580–7586.